SIMULATION OF THE CLIC BEAM DELIVERY SYSTEM USING BDSIM

G.A. Blair*

Abstract

This note describes the simulation of the CLIC beam delivery system (BDS) using a Geant4 [1] based program BDSIM. BDSIM is designed flexibly in order to track particles through the BDS of a generic linear collider and includes particle interactions and production of secondaries in materials. The code itself is described in Section 2 and this note serves as initial documentation for the programme. The detailed input to the program is controlled by an optics file and cards file, described in Section 10 and Section 11 respectively and the processes present are outlined in Section 4. Results are presented for the tracking performance of the program (Section 3) and its use in determining the backgrounds from halo particles (Section 5); particular emphasis is placed on the determination of muon production rates (Section 6) due to halo loss upstream of the interaction point (IP). Some earlier studies of energy deposition in spoilers are also included for completeness in Section 7. The simulation of a laserwire system is introduced in Section 8.

*) Royal Holloway University of London, UK/CERN

CLIC Note 509: Simulation of the CLIC Beam Delivery System using BDSIM

Grahame A. Blair, Royal Holloway Univ of London, UK./CERN

September 20, 2002

1 Introduction

This note describes the simulation of the CLIC beam delivery system (BDS) using a Geant4 [1] based program BDSIM. BDSIM is designed flexibly in order to track particles through the BDS of a generic linear collider and includes particle interactions and production of secondaries in materials. The code itself is described in Sec. 2 and this note serves as initial documentation for the programme. The detailed input to the program is controlled by an optics file and cards file, described in Sec. 10 and Sec. 11 respectively and the processes present are outlined in Sec. 4. Results are presented for the tracking performance of the program (Sec. 3) and its use in determining the backgrounds from halo particles (Sec. 5); particular emphasis is placed on the determination of muon production rates (Sec. 6) due to halo loss upstream of the interaction point (IP). Some earlier studies of energy deposition in spoilers are also included for completeness in Sec. 7. The simulation of a laserwire system is introduced in Sec. 8.

2 The BDSIM Code

The BDSIM code uses Geant4 to build the individual beamline elements including drifts, sector bends, quadrupoles, sextupoles, octupoles and decapoles. Adopting the object oriented approach, each beamline element is constructed as a separate object with its own outer geometry, beampipe and magnetic fields. The input to the program is currently in the form of a MAD optics file, discussed in Sec. 10. This format was chosen to allow the program to be used easily with a range of BDS designs for comparative studies. All the dimensions and parameters are entered into the program via a simple cards file described in Sec. 11; in this way the program can be used easily in comparative studies of BDS layouts and parameters without recompiling.

At present the individual properties such as bunch charge and beam energy are defined within the file BDSAcceleratorType.cc. The relevant machine can then be chosen by the card ACCELERATOR and the type of bunch (halo or normal) by the card BUNCH_TYPE.

Inside the beampipe a new approach is adopted. Rather than track the particles using a locally defined magnetic field strength, the approach more commonly adopted by accelerator tracking codes is followed, using an analytic solution to the equations of motion. For example, the track of a particle moving in a uniform magnetic field describes a circle, so the solution to the equation of motion is known and does not need to be solved locally. Similarly a particle moving in an idealised quadrupole field has equations of motion with an analytic solution. By using the analytic solutions directly, a significant time saving is obtained over the more usual Geant approach of solving locally for a step in a magnetic field. Of course, this is only useful when the magnetic fields have a simple form. The approach is illustrated schematically in Fig. 1

For higher order multipoles such as sextupoles, octuples, or decapoles, a simpler approach is adopted where the particles receive a momentum kick dependent on their position on entering the multipole. This approach, also common in accelerator physics, works well enough for the purpose of tracking through the BDS.

The implementation of this accelerator style tracking is performed through the use of dedicated "steppers". In practice this is effected by assigning each "logical volume" its own stepper so that when a particle enters that volume it automatically picks up the stepper of that volume, which in turn determines how the particle is transported. Given a particle of energy E and input transverse position x, y with respect to the longitudinal position along the beampipe, z, and angles x', y' with respect to the distance travelled (Δs) the final co-ordinates can be determined directly within the stepper. The magnitude of
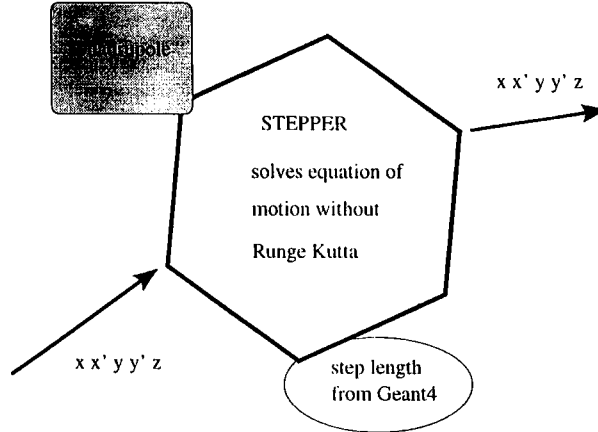
1

Figure 1: The simple concept of how accelerator-style tracking is incorporated in BDSIM. Any component, in this case a quadrupole, has its own stepper. Geant4 provides the step length (whose value depends on the mean free path from the active processes) and, given this step length, the stepper provides the final position and trajectory as given analytically for the case of quadrupoles and sector bends, or approximately via momentum kicks for higher order multipoles.

the step length Δs is provided by the Geant4 code and depends on which processes are present (these are described in more detail in Sec. 4). For most cases, the step length is equal to the length of the beamline element because the particles are travelling in high vacuum. However, for studies with finite pressure or with the inclusion of synchrotron radiation, the step length will vary from step to step, with distributions given by the mean free path of the process involved. Scattered particles, or those halo particles in outer positions of phase-space, can leave the beampipe. Once outside the beampipe, tracking defaults to the usual Geant approach where steps are calculated from local fields (if present) using Runge-Kutta techniques and material interactions are included in full.

The magnetic field in the material of the magnets is calculated as follows. The field at the pole-tips is determined from the analytic and idealised multipole field equation. The magnetic flux is then conserved through the iron of the magnet, so that the magnitude of the field is a simple ratio of the cross-sectional area of the iron to that of the pole tip. This approach is illustrated in Fig. 2 for the case of a quadrupole. All the dimensions of the magnets, such as outer radius of iron, R_o, inner radius of iron R_i, thickness of iron $T = R_o - R_i$ and pole-tip transverse dimension P are entered via the cards file. The magnetic field in the iron is calculated as $B = B_{\text{pole}} * P/T$, where B_{pole} is the field at the pole-tip, as calculated from the ideal field distribution of the multipole at that position. Physical poles are not yet included in order to keep geometries as simple as possible; but it would be easy to include them if necessary.

3 Tracking Results

The tracking performance was tested in detail as part of a comparison of a wider set of tracking codes [2]. A test sample of 20k normal beam particles was tracked through the long (6 km) CLIC 1.5 TeV-per-beam baseline design. The results in terms of the spot-size at the IP are shown in Tab. 1.

The results agree very well with the other tracking codes described in Ref. [2], with the possible exception of tracking with synchrotron radiation (SR), where some small discrepancies remain. However the treatment of SR varies from code to code and the RMS spot size is very dependent on the details of long tails in the distributions. The main conclusion to draw from Tab. 1 is that the tracking works well-enough to describe the 1.5 TeV electron trajectories over 6 km at the sub-nm level and gives confidence that the tracking code can be used reliably for the determination of backgrounds and for optimisation of the BDS layout.

4 Processes

BDSIM has easy access to all the impressive range of processes that are included in the Geant4 package. These processes include multiple scattering off beam-gas particles or in detector elements and the usual electromagnetic shower processes such as electron-positron pair creation and bremsstrahlung. The beam-
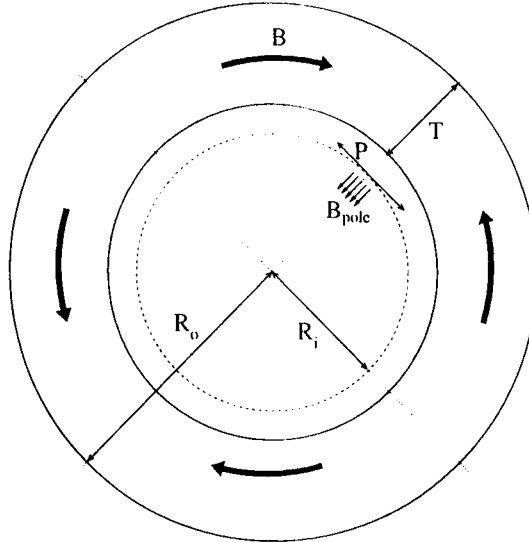
2

Figure 2: The field distributions assumed for the outer material in beamline elements. The magnitude of the fields in the iron is calculated by simple flux-conservation considerations. See text for details.

	ϵ (nm)	Program	DE=0, No SR	DE, no SR	DE & SR
H	680	BDSIM	42.96±0.10	48.06 ± 0.11	59.33 ± 0.13
H	680	Placet	42.93±0.07	47.97 ± 0.05	58.92 ± 0.15
V	20	BDSIM	1.013±0.003	1.33 ± 0.03	2.44 ± 0.03
V	20	Placet	1.012±0.001	1.30 ± 0.02	2.25 ± 0.05
V	10	BDSIM	0.716± 0.002	0.93±0.02	1.75 ±0.03
V	10	Placet	0.715± 0.001	0.91±0.01	1.51 ±0.02

Table 1: Horizontal (H) and vertical (V) spot sizes after tracking a nominal bunch along the CLIC baseline BDS for two values of the CLIC emittance ϵ. The cases with flat energy spread DE= ±1% and DE=0 are included as are the case of DE= ±1% together with synchrotron radiation (SR). For comparison, the results obtained with Placet [7] are also included.(Further comparisons are presented in Ref. [2]).

gas is specified by a normal Geant4 material with a pressure that can be defined by the user. Neutron generation from photo-production can also be included using the Geant4 nuclear processes [4].

The usual material interactions are provided by the Geant4 routines. The full simulation of electromagnetic showers in the TeV range can be very time consuming, so a cut-off is implemented to stop any charged particles with energies less than this cut. The value of this cut is set by the card THRESHOLD_CUT_CHARGED which is set at 10 GeV for the studies presented in this note. Similarly a cut is provided to stop photons via the card THRESHOLD_CUT_PHOTONS, which is set at 10 MeV for the following studies.

Synchrotron radiation (SR) can be included (set by the cards file) so that generation of synchrotron photons from electrons in the magnet elements is performed. Subsequent tracking of these photons is of course also possible and is controlled by a switch in the cards file. An example of SR generation and tracking is shown in Sec. 5. An additional option set by the card RESCALE_DUE_TO_SYNCHROTRON will determine the energy loss due to SR in each element and rescale the strength of subsequent elements accordingly. This option has a cost in terms of memory, because it results in every similar element being created separately with its own multipole field strength. When this option is not set, all similar elements have one Geant4 logical volume that is used whenever the element is needed; in other words there is one element in memory that is used several times during a single event. For most purposes, this option should be turned off; the only time it is needed is for detailed tracking studies including SR.

An example of the default Geant4 showering and subsequent tracking in BDSIM was presented in Ref. [5] and is shown in Fig. 3(left). In this case the off-energy bunch was generated by the program PLACET [7], for which a dedicated interface was written.

Additional processes have been included as options. A Compton scattering process has been developed for use in describing laser-wire processes, discussed in some detail in Sec. 8, where light from a laser is
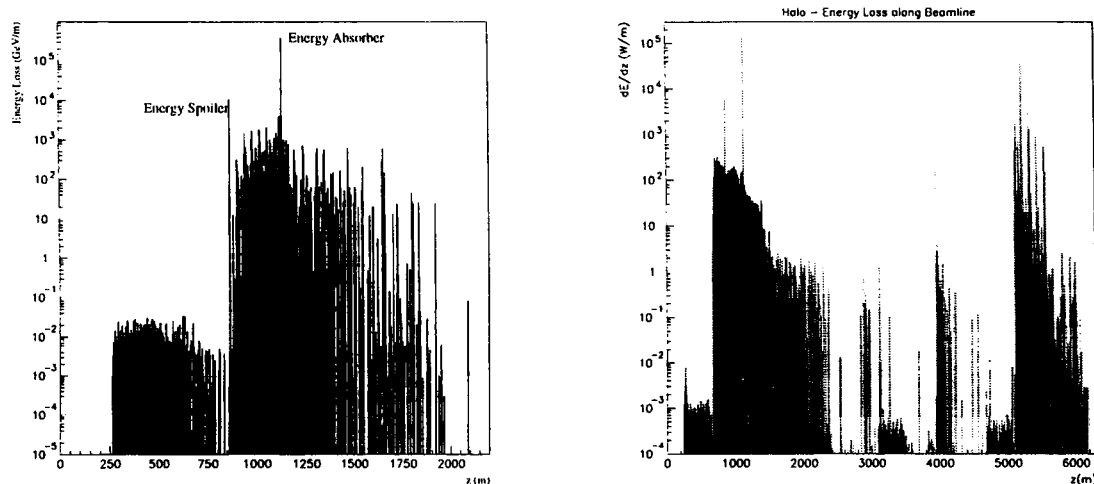
Figure 3: Left: energy loss as a function of z for a bunch that is offset in energy by -2 %. The low-level of energy loss before the energy spoiler is due to synchrotron radiation. The deposition of energy downstream is dominated by absorption in the absorber and, to a lesser extent, the spoiler. Right: total energy loss for the halo described in Tab. 2 as a function of position along the BDS for the CLIC long baseline design. 10^5 initial halo particles were used in this simulation and the normalisation in this plot assumes that the halo is 10^{-3} of the nominal bunch charge.

scattered by the incoming electron beam. Subsequent tracking of the scattered photon and electron is natural in this approach. Similarly the Compton scattering of electrons off thermal photons in the vacuum has been included as a option, which is set by the the card TURN_ON_PLANCK.

5 Halo Studies

The baseline 6 km CLIC BDS design was studied for its efficiency in reducing beam halo. For the purposes of this study, the halo was defined by uniform distributions in phase-space variables according to the parameters defined in Tab. 2

Bunch parameter	Range
x	$10. \times 1.25 \times \sigma_x$
y	$70. \times 1.25 \times \sigma_y$
x'	$10. \times 1.25 \times \sigma_x$
y'	$70. \times 1.25 \times \sigma_y$
E	$(0.98 - 1.02) \times E_0$

Table 2: Parameters defining flat distributions to describe the CLIC beam halo

Some preliminary results are shown in Fig. 3(right) where the energy loss due to 10^5 halo particles is shown and the plot is normalised to be equivalent to a beam halo with bunch charge 10^{-3} of the nominal bunch charge. Most of the particles are absorbed in the spoilers (consisting of one radiation length of graphite) and absorbers (consisting of 35cm of copper); however additional losses due to synchrotron radiation or other particles leaving the beampipe are also apparent. A cut of 10 GeV was applied to charged particles in the EM showers. Figure 4 shows the electronic energy remaining in the halo as a function of position along the BDS.

Tracking the secondaries along the BDS results in the spatial and energy distributions shown in Figs. 5, 6, 9, the latter being discussed in more detail in Sec. 6.
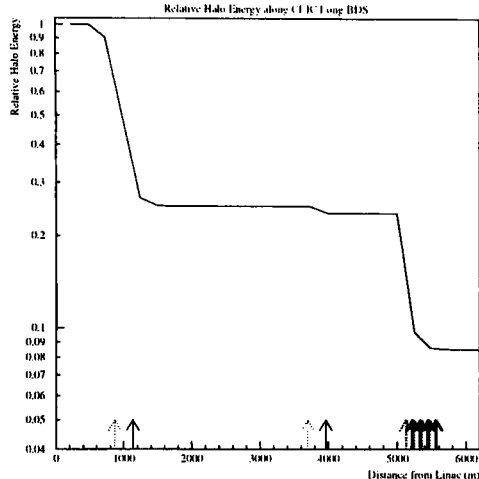
4

Figure 4: Relative summed total energy of the electrons in the halo along the CLIC long BDS. The dotted arrows mark the positions of the spoilers and the solid arrows the positions of the collimators. The remaining energy passes through the IP, because some of the flat halo distribution is within the acceptance of the BDS.

6 Muon Generation in the BDS

A new physics process, photon conversion to muon pairs, has been incorporated into the standard Geant4 release [3]. This process allows muon production in electromagnetic showers and their subsequent tracking through the tunnel. The energy distribution of muons produced by this process from a 1.5 TeV electron incident on a shower-absorber combination is shown in Fig. 7(left).

As discussed in Sec. 2, at present BDSIM models the beam-line elements as cylinders of iron with an optional simple description of magnetic fields within the iron. This simple description takes the multipole pole field and distributes the magnetic flux uniformly as rings in the iron. Preliminary results are shown in Fig 8(left).

In the study presented in Fig. 8 electromagnetic showers were cut off when particles have energy 10 GeV or less. In addition the muon production cross section was increased by a factor of 10^3 in order to improve statistics. This is discussed further below. In order to make contact with previous studies, the effect of cutting off the shower after the primary bremsstrahlung photon in the shower is also shown. The tunnel was modelled as a cylinder of concrete with inner radius 2m and outer radius 4m. The first conclusions to be drawn from Fig 8 are that the magnet element geometries are the most important factors in determining the muon flux at the detector. The effect of the magnetic fields in the iron seems to be of order 40%.

The effect of the factor 10^3 is shown in Fig 7(right) where electrons of energy 1.5 TeV are fired at a spoiler and absorber placed next to each other. The shower is essentially completely contained within the spoiler/absorber material. The plot shows that setting the cross-section multiplication factor at 10^3 seems a reasonable balance between statistics and bias; the total number of muons produced and their mean energy are within 10% of the unscaled values. Some caution is required here, because the dangerous muons are in the high energy tail, which could be affected by such a scaling factor. However the effect of a scaling factor is to bias towards more high energy muons, so including a factor is tending towards conservatism. The muon pair production rate is a factor $\sim 10^{-5}$ that of electron production, so scaling factors should be small compared to $\sim 10^5$. So, for future high statistics runs a factor of 10^2 is probably the best, as used in the halo study described above.

Using a muon scaling factor of 100, the production rate of muons after the spoiler and also after the spoiler/absorber pair, are given in Tab. 3.

Fig. 9 shows the transverse distribution of muons after production in the beam-line elements (mostly spoilers and absorbers) and their subsequent tracking down the 6 km tunnel. A scaling factor for the muon production cross section of 100 was used here which, as shown in Fig. 7, is safe for our purposes. A concrete tunnel extending from a radius of 2 m out to a radius of 20 m was assumed (effectively assuming the earth to be similar to concrete for the purposes of muon tracking). A default component diameter of
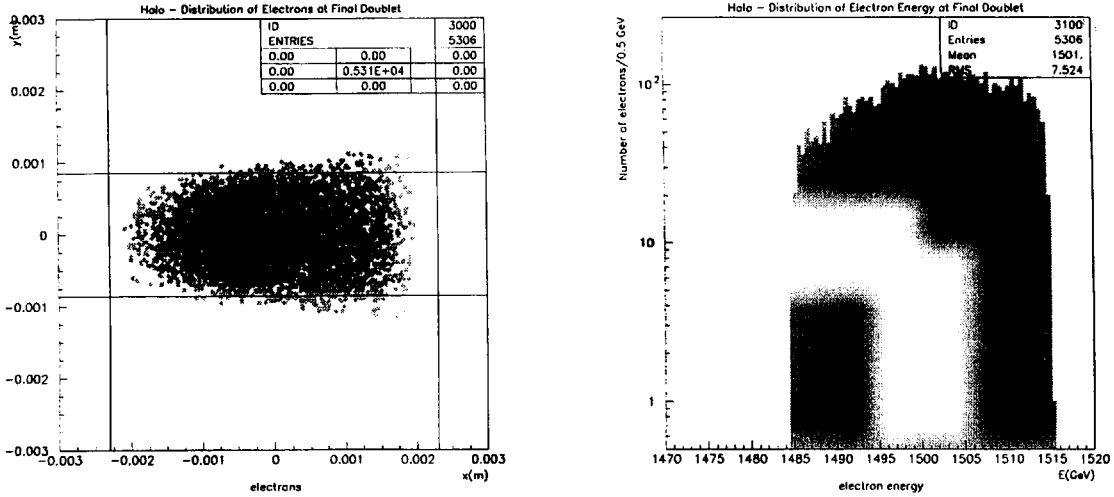
Figure 5: Left: Spatial electron halo distribution at the entrance to the final doublet. 10^5 events were generated at the entrance to the BDS, with the phase-space distribution given by Tab. 2. The lines show the nominal collimation depth of the system. Right: The corresponding electron energy distribution.

E_{beam}	N_{sp}	$E_{\text{sp}}^{\text{mean}}$	$N_{\text{sp+abs}}$	$E_{\text{sp+abs}}^{\text{mean}}$
250	$(3.8 \pm 0.6) \times 10^{-5}$	22	$(4.4 \pm 0.2) \times 10^{-4}$	11
1500	$(6.6 \pm 0.8) \times 10^{-5}$	101	$(2.65 \pm 0.05) \times 10^{-3}$	24

Table 3: Rates of muon production and mean muon energy for electrons that hit a spoiler (sp) and absorber (abs) pair. The numbers are normalised to the rate for one incident electron and all energies E are in GeV. Values are given for just after the spoiler only and also for just after the absorber.

20 cm was also assumed, the effect of which can be important (see Fig. 8: left). The positions where those muons, which make it to the detector, are produced via beam halo interaction with beamline elements are shown in Fig. 8(right).

The main result from Fig 9 is that $(2.02 \pm 0.14) \times 10^{-5}$ muons are produced and survive to the detector per initial halo particle. This means that for a halo level of 10^{-3} of the nominal bunch charge of 4×10^9, a train of 154 bunches would produce $(1.24 \pm 0.09) \times 10^4$ muons in the detector. The effect of such muons in the detector has been described in Ref. [6].

7 Geant Simulation of Spoilers

For completeness, some early studies are reported here where Geant3 was used to determine the energy deposition in a spoiler for CLIC beams. In these simulations electrons of energy 1.5 TeV were fired at a spoiler and the energy deposited as a function of position was counted for two candidate spoiler materials, titanium and carbon (graphite). The assumed beam parameters at the spoiler are given in Tab. 4

The energy density deposition at the very centre of the beam was obtained by considering a rectangular volume of transverse dimensions σ_x and σ_y positioned coaxially with the bunch trajectory as shown in

Parameter	CLIC
Beam Energy	1.5 TeV
Number of particles per bunch	$4. \times 10^9$
Gaussian bunch size at spoiler: σ_x	726 μm
Gaussian bunch size at spoiler: σ_y	27.8 μm
Maximum number of bunches on spoiler:	154

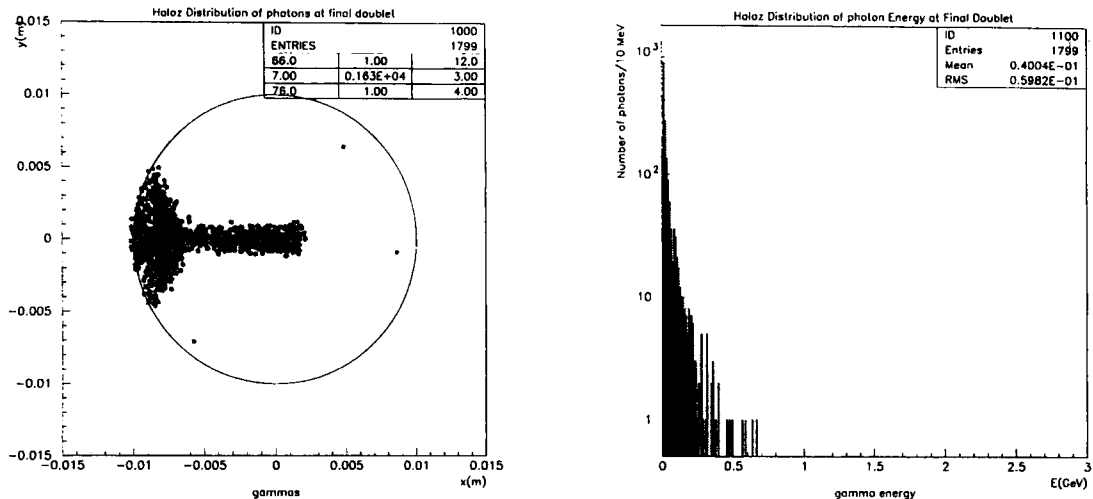Table 4: The bunch parameters used in the Geant3 spoiler simulations.

Figure 6: Left: Spatial gamma halo distribution at the entrance to the final doublet. 10^5 events were generated at the entrance to the BDS, with the phase-space distribution given by Tab. 2 Right: The corresponding photon energy distribution.

Fig. 10. The results are shown in Fig. 11.

The results show the expected form, where initially the energy deposition is flat, due to the dE/dx of the incoming minimum ionising electron. Once the shower starts, a rapid rise in energy deposition takes place as more electrons contribute their dE/dx. Eventually, as can be seen in the case for carbon, the shower energy density within the core of the beam starts to flatten out (and eventually falls) as the rate at which the shower spreads out more than compensates for the increase in electron number.

Whether a spoiler can withstand this energy deposition is fundamentally an experimental issue that needs to be tested in a realistic beam. However a first idea can be obtained by considering the ultimate tensile stress (UTS) limit, which is given by the maximum instantaneous local temperature rise that the material can withstand. The relevant numbers for carbon and tungsten are given in Tab. 5 and the corresponding limits for the spoiler are indicated by arrows on Fig 11. The results indicate that one-radiation length carbon spoilers could withstand of order 800 consecutive bunches at one position, whereas titanium could withstand only 70 such bunches. For this reason, a one-radiation length graphite spoiler was assumed in the BDS simulations.

Material	$\Delta T_{\mathrm{UTS}}(K)$	$(dE/dm)_{\mathrm{max}}(J/g)$
Titanium	1000	635
Carbon	2650	5100

Table 5: The maximum instantaneous energy deposit that the spoiler can withstand, based on the maximum instantaneous temperature change from ultimate tensile strength (UTS) considerations.

8 Laser-wire Simulation

BDSIM includes a component called LASERWIRE that forces any incoming electron to Compton scatter off a laser photon. The direction and wavelength of the laser beam can be specified in the cards file. Either the scattered electron only, or the photon only, or both the electron and the photon can be tracked further down the BDS. This allows the position of the laserwire to be optimised and will enable the best way to extract the signal to be determined. An introduction to the principle and theory of laserwires can be found in Ref. [8].

The Compton cross section σ_C is related to the Thomson scattering cross section $\sigma_0 = 6.65 \times 10^{-25} \mathrm{cm}^2$ by Eqn. 1:
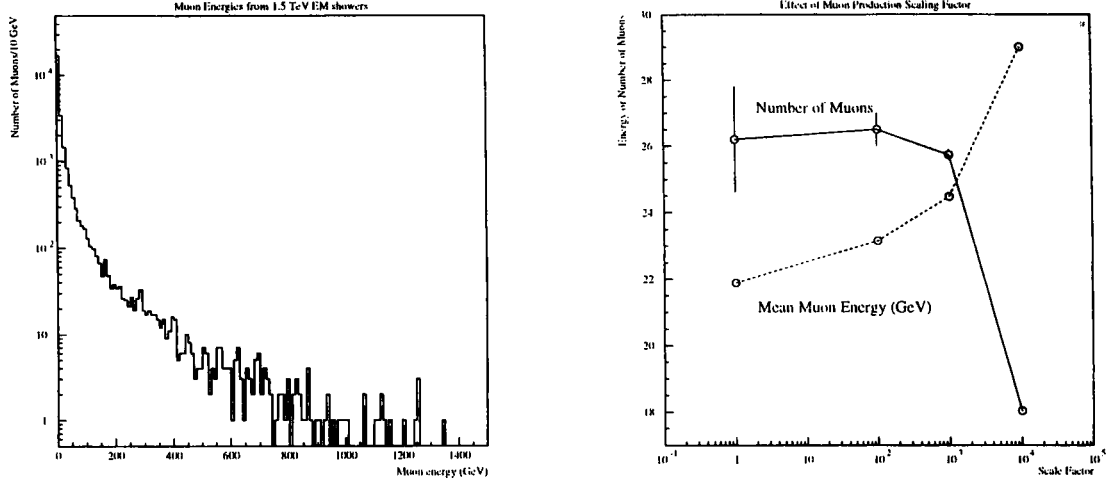
Figure 7: Left: energies of muons produced in from a 1.5 TeV electron beam incident on a shower-absorber combination, using the Geant4 process for muon pair production from photons. Right: The effect of the muon cross-section scaling factor on the total number of electrons produced in a spoiler/absorber pair and on the mean energy of these muons. The initial electrons have energy 1.5 TeV.

$$\sigma_C = \sigma_0 \frac{3}{4} \left\{ \frac{1+\epsilon}{\epsilon^3} \left[\frac{2\epsilon(1+\epsilon)}{1+2\epsilon} - \ln(1+2\epsilon) \right] + \frac{1}{2\epsilon} \ln(1+2\epsilon) - \frac{1+3\epsilon}{(1+2\epsilon)^2} \right\} \tag{1}$$

where $\epsilon = \gamma \frac{\omega_0}{m_e}$ is the normalised energy of the laser photons in the electron rest frame and γ is the Lorentz factor associated with the incident electron beam energy E_b ($\gamma = \frac{E_b}{m_e}$). The energy spectrum of the emerging gamma rays is given by Eqn. 2:

$$\frac{d\sigma}{d\omega} = \frac{3\sigma_0}{8\epsilon} \left\{ \frac{1}{1-\omega} + 1 - \omega + \left[\frac{\omega}{\epsilon(1-\omega)} \right]^2 - \frac{2\omega}{\epsilon(1-\omega)} \right\} \tag{2}$$

In the following we consider an electron bunch with a Gaussian distribution of particles in the plane transverse to the bunch velocity, as illustrated in Fig. 12. The transverse dimension we are interested in measuring is σ_b which must be aligned perpendicular to the direction of the laser beam. The setup is illustrated in Fig. 12(a) The laser beam is focused to a small Gaussian spot with an RMS size σ_f which, for a diffraction-limited laser beam is given by

$$\sigma_f = \frac{\lambda f_\ell}{4\pi\sigma_\ell} \tag{3}$$

where f_ℓ is the focal length of the optics which is focusing the laser down to the small spot size and σ_ℓ is the RMS spot size of the beam when it leaves the laser. The useful depth z_R (the Raleigh range) of laser beam is given by Gaussian beam optics to be:

$$z_R = \frac{4\pi\sigma_f^2}{\lambda}. \tag{4}$$

We will require that the laser pulse lasts longer than the time taken for one bunch to pass through it. In the case of CLIC the 30 μm RMS bunch lengths will require minimum laser pulse lengths of approximately 100 fs, synchronised with the electron bunch. Now that the entire electron bunch sees the laser beam, the number of Compton photons per electron bunch is given by:

$$N_\gamma = N_b \frac{P_L \sigma_C \lambda}{c^2 h} \frac{1}{\sqrt{2\pi}\sigma_s} \exp\left(\frac{-y^2}{2\sigma_s^2} \right) \tag{5}$$

where N_b is the number of electrons per bunch and $\sigma_s^2 \equiv \sigma_b^2 + \sigma_f^2$. The relative transverse offset between the bunch and the laser spot is given by y, as illustrated in Fig. 12(b).
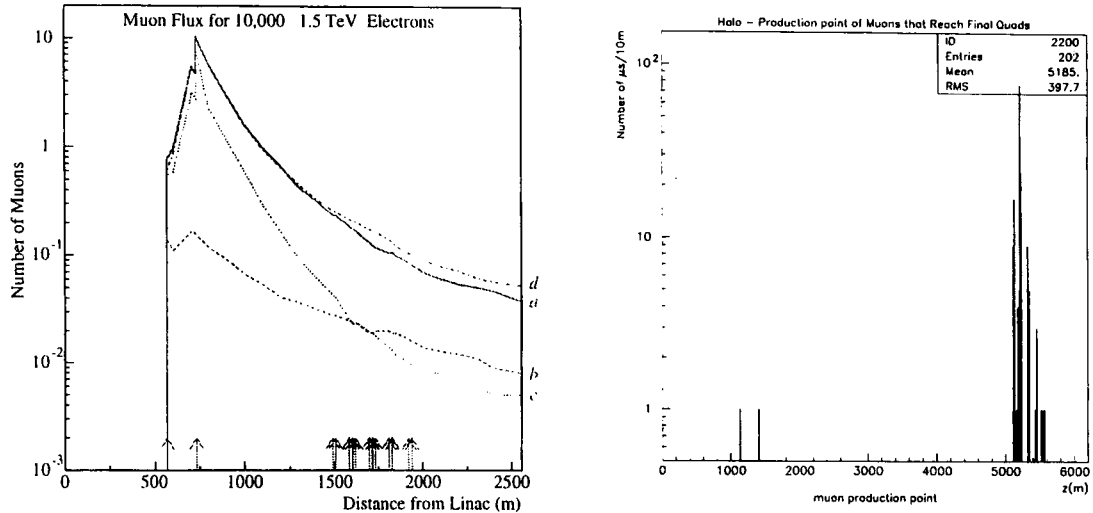
Figure 8: Left: Muon flux determination from Geant4 for a 1.5 TeV beam with a -2% offset in energy. The positions of the spoilers and collimators are shown by arrows. Case a corresponds to magnet elements consisting of unmagnetised (and case d magnetised) cylinders of iron of diameter 20 cm with fully simulated showers, case b for the case with only the first photon of a shower contributing. Case c is the same as case a except that magnet elements have diameter 50 cm. Right: The position along the BDS where muons are produced by interaction of beam halo with beamline elements and subsequently reach the detector after tracking through the tunnel.

In the following we assume that approximately 1000 Compton events are obtained for each laser shot (these numbers are justified further in Ref. [9]). One of the major challenges of a laserwire system is to extract the Compton photons, or electrons, in an already crowded BDS. At the point of the laserwire, the energy distributions are shown in Fig. 13 for the scattered electrons (left) and the photons (right). These particles were subsequently tracked using BDSIM and the resulting energy deposition as a function of length along the BDS is displayed in Fig. 14(left).

In the BDS the profile measurement will be made by measuring the total energy in a calorimeter stationed somewhere along the beamline. By firing 100 laserwire events, each of 1000 Compton scatters, the fluctuations in the signal between events can be determined. The results are shown in Fig. 14 (right). Here it can be seen that the fluctuations are large because the energy of the event is scattered over a long region. This effect would severely limit the intrinsic performance of the laserwire which, if it is to provide a fast and accurate profile measurement, needs to make use of as much of the scattered energy as possible.

A potential solution to this problem could be provided by installing dedicated calorimeters close to the beam, assuming that issues such as radiation hardness and wake field generation could be overcome. In addition, the question of backgrounds due to beam halo needs to be considered and, referring to Fig. 3, these losses can be substantial and will restrict the choice of location of the laserwire. These issues are discussed in more detail in Ref. [9].

9 Sampler Object and Output

In order to sample the beam, a BDSSampler object has been created. This has very small length (effectively zero) and can be placed at any point along the BDS. Whenever a particle traverses the BDSSampler, its particle type, energy, position and momentum and event number are logged in addition to its original momentum and position on entering the BDS. The exception are muons whose original momentum and position are defined as those at the point of creation of the muon. In version 1.0 of BDSIM, the particle properties are stored in PAW ntuples. It is planned to move to an object-oriented storage environment, such as ROOT in the near future.

An example output ntuple is shown here:

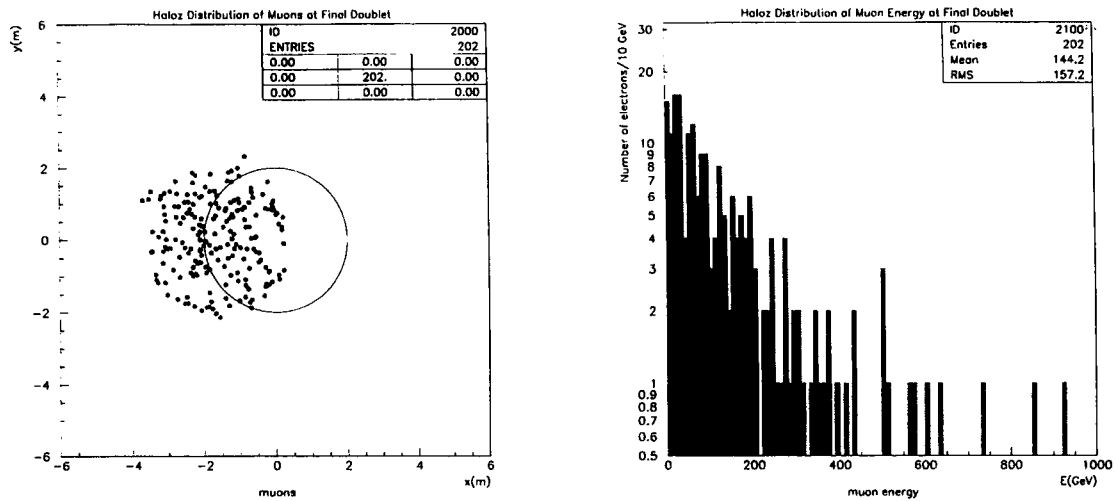**

Figure 9: Left: Spatial muon halo distribution at the entrance to the final doublet of the long version of the 3 TeV CLIC BDS. 10^5 events were generated at the entrance to the BDS, with the phase-space distribution given by Tab. 2 and muon scale-factor = 100 and the showers cut at 10 GeV The tunnel cross section at the final doublet is also shown as a circle. Right: The corresponding muon energy distribution.
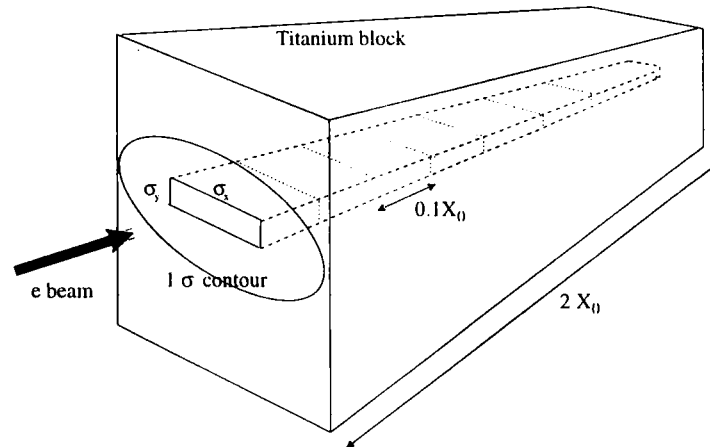

Figure 10: The setup used in the Geant3 simulation of spoilers

```
* NTUPLE ID=      1  ENTRIES=     1000
*************************************************************
*  Var  numb  *   Name   *    Lower    *    Upper    *
*************************************************************
*        1    * x0       * -.892904E-05 * 0.103764E-04 *
*        2    * xp0      * -.351638E-06 * 0.374634E-06 *
*        3    * y0       * -.716920E-06 * 0.851532E-06 *
*        4    * yp0      * -.572486E-07 * 0.400196E-07 *
*        5    * E0       * 0.149250E+04 * 0.150749E+04 *
*        6    * z0       * -.166016E-03 * 0.254512E-03 *
*        7    * x        * -.177289E-04 * 0.197849E-04 *
*        8    * xp       * -.518513E-06 * 0.559182E-06 *
*        9    * y        * -.353297E-05 * 0.384535E-05 *
*       10    * yp       * -.136618E-06 * 0.312452E-06 *
*       11    * E        * 0.149240E+04 * 0.150744E+04 *
*       12    * z        * -.476788E-03 * -.566012E-04 *
*       13    * part     * 0.110000E+02 * 0.110000E+02 *
```
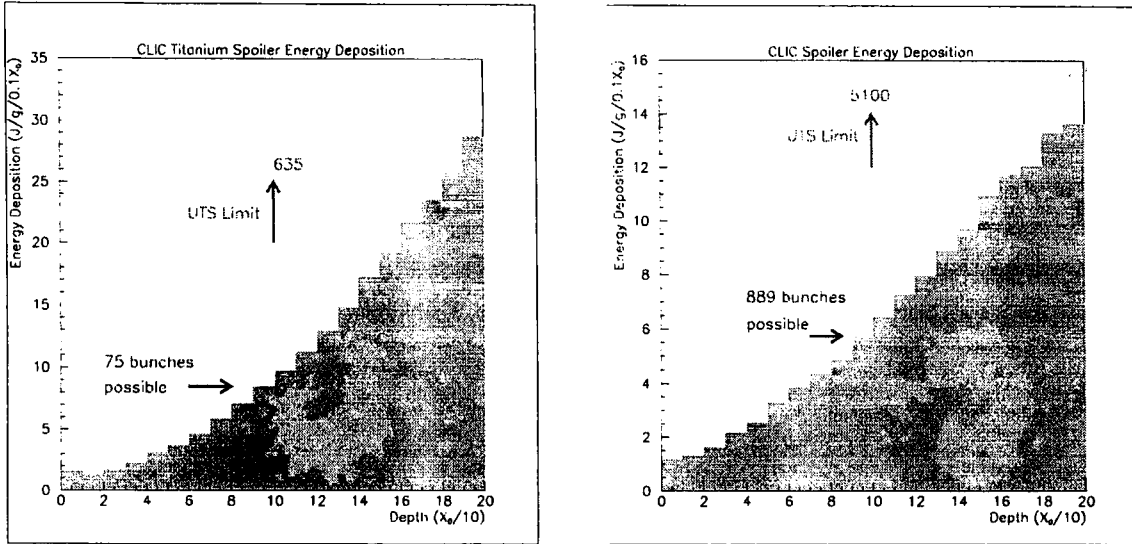
Figure 11: Energy distribution resulting from a 1.5 TeV electron bunch incident on a spoiler. The left hand plot shows the case for titanium and the right hand plot that for carbon.
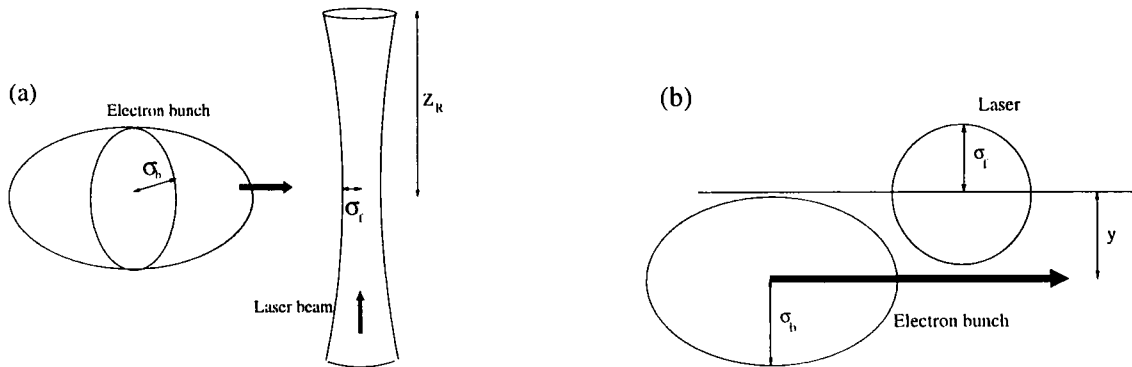

Figure 12: *Setup showing the definition of the laser beam and beam spot dimensions relevant to this analysis. (a) Shows a side view; note that it is the dimension of the beam spot perpendicular to the laser beam that is denoted by σ_b. (b) View from the top, showing an offset y between the centre of the bunch and the centre of the laser beam.*

```
*      14      * nev        * 0.200000E+04 * 0.299900E+04 *
**********************************************************
```

The output file has a name defined in the input cards file (Sec. 11) to which is appended the string _N where N is the number of the file in a large batch run. The number of events in each file is also defined in the cards file and, when that number has been generated, the output file is closed and a new one created, with N incremented. In this way, the batch can be protected against crashes by saving the results already made.

Also included in the standard output file are two histograms with number 100 and, if the card USE_EM_HADRONIC is set, 101. Histogram 100 contains one bin for each metre of BDS and logs the total energy lost within that length. Examples of these histograms for the energy loss due to an off-energy bunch and that due to halo are shown respectively in in Fig. 3(left) and (right). The histogram 101 shows the position at which a neutron, generated via the Geant4 photo-nuclear processes, enters the beampipe vacuum.

10   Input Optics File

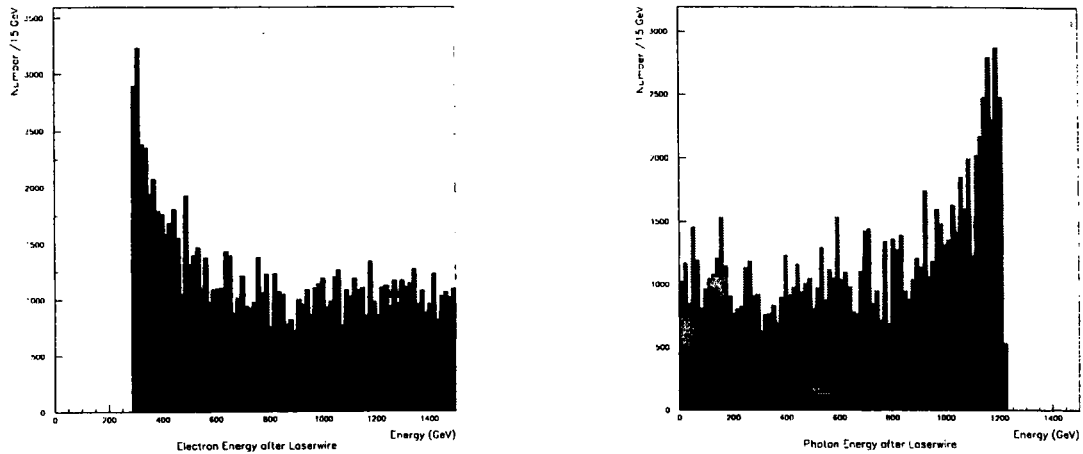The current input file format is illustrated below:

Figure 13: The energy distributions for electrons (left) and photons (right) after Compton scattering in the laserwire.

* NAME	KEYWORD	S	L	K0L	K1L	K2L	K3L	K4L	TILT	TYPE
$ %16s	%16s	%e	%e	%e	%e	%e	%e	%e	%16s	
@ XIY	%e	9.79550								
@ XIX	%e	-1.53072								
@ QY	%e	7.96069								
@ QX	%e	5.14820								
@ CIRCUM	%1e	6185.97556104								
@ DELTA	%e	0.000000E+00								
@ TYPE	%08s	"OPTICS"								
@ COMMENT	%36s	"L== 4.3 m, Bx** 0.8 cm, By** 0.15 mm"								
@ ORIGIN	%16s	"MAD 8.51/07 Unix"								
@ DATE	%08s	"22/08/01"								
@ TIME	%08s	"11.50.09"								
"BDS"	"LINE"	0.000000E+00	0.000000E+00	0.000000E+00	0.000000E+00	0.000000E+00	0.000000E+00	0.000000E+00	0.000000E+00	"-"
"LTCD0"	"DRIFT"	35.4240	35.4240	0.000000E+00	0.000000E+00	0.000000E+00	0.000000E+00	0.000000E+00	0.000000E+00	"-"
"LTCQ1"	"QUADRUPOLE"	40.4240	5.00000	0.000000E+00	-0.125100	0.000000E+00	0.000000E+00	0.000000E+00	0.000000E+00	"-"
"LTCD1"	"DRIFT"	45.1900	4.76600	0.000000E+00	0.000000E+00	0.000000E+00	0.000000E+00	0.000000E+00	0.000000E+00	"-"
"LTCQ2"	"QUADRUPOLE"	50.1900	5.00000	0.000000E+00	0.994664E-01	0.000000E+00	0.000000E+00	0.000000E+00	0.000000E+0	

Of particular importance to the definition of apertures:

"ENGYSP"	"SPOILER"	566.502	0.188510E+00	0.000000E+00	0.000000E+00	0.000000E+00
"DLPA2"	"DRIFT"	187.670	1.75000	0.00000	0.00000	0.00000

Where the term "X8Y20" refers to an aperture of total width 8 mm in x and 20 mm in y (i.e. half-width 4 mm and 10 mm respectively) and the second term "D20" refers to a circular aperture of diameter 20mm. A ~ refers to a default beampipe radius, defined within the cards file. Similarly "H20" refers to an SBEND total gap height of 20 mm.

11 Input Cards File

The code is controlled by a simple ASCII cards file, an example of which is listed below. Some of the cards have been described above, others should be obvious from the associated comments below.

```
* Input cards for Beam Delivery System Simulation
*
* ==================================================
*             >>> Accelerator <<<
ACCELERATOR clic
* ACCELERATOR tesla
* BUNCH_TYPE    halo
BUNCH_TYPE    normal
READ_BUNCH_FILE 0
EXTRACT_BUNCH_FILE 0
WRITE_BUNCH_FILE 0
*
* Generic Output Ntuple File Name (will have _N.rz appended for integer N) :
* (Default is sampler_output.rz)
```
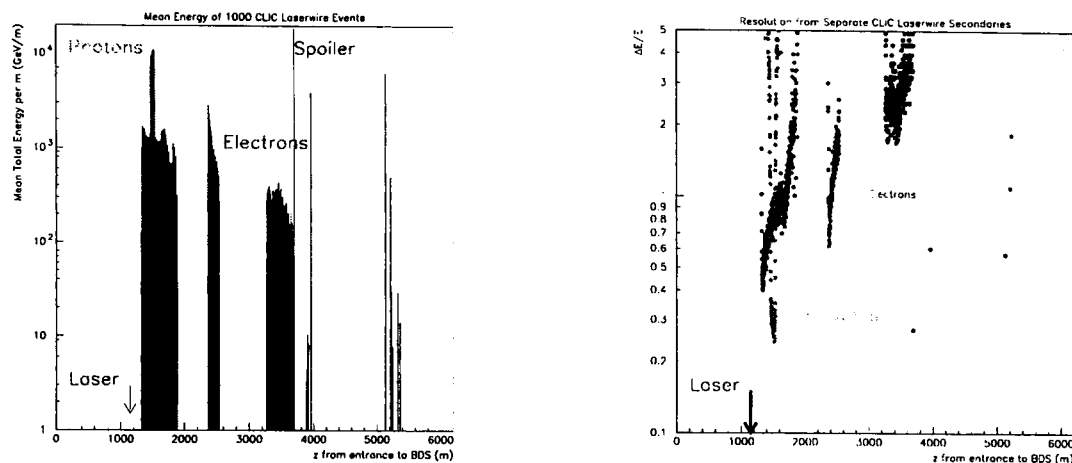
Figure 14: Left: the energy distribution along the BDS resulting from 1000 Compton scatters. Shown in red (light grey) are the energy deposits per m from the scattered photons and in blue (dark grey) the energy deposits from the scattered electron. The laser wavelength used in these studies is 532 nm. Right: the intrinsic relative fluctuations in the energy deposits arising from the Compton process as a function of position along the BDS.

```
OUTPUT_NTUPLE_FILE_NAME
clic_normal
* Number of events to include per file; insurance against crashes during batch.
* a new file is created _(N+1).rz after this number of events
NUMBER_OF_EVENTS_PER_NTUPLE
1000
* =========================================================
* Batch Conditions
* Set to true if you want to run in batch mode (no visualisation)
USE_BATCH 0
* Number of events to generate in the run:
NUMBER_TO_GENERATE 10
* Random Number Seed
RANDOM_SEED
100000
* =========================================================
*
* Energy offset of bunch (GeV) - for collimation studies
ENERGY_OFFSET 0.0
* =========================================================
*                >>> Tracking Parameters <<<
* Energy below which charged particles are stopped: (in GeV)
THRESHOLD_CUT_CHARGED 10.
*
* Energy below which photons are stopped: (in GeV)
THRESHOLD_CUT_PHOTONS 0.001
*
* Weighting factor for tracks crossing weighting planes
TRACK_WEIGHT_FACTOR 1.
*
* Turn on interactions; 0 leaves only transportation
* (or planck or synchrotron radiation or laserwire, if set)
TURN_ON_INTERACTIONS 1
* =========================================================
*                >>> Basic Dimensions <<<
* Default values
* size of typical box dimensions transverse to the beamline axis (in cm):
ACCELERATOR_COMPONENT_BOX_SIZE 20.0
```

```
* size of magnet poles (in cm):
MAGNET_POLE_SIZE 1.0
* radial position of magnet poles (in cm):
MAGNET_POLE_RADIUS 2.0
*
* Radius of tunnel (in m):
TUNNEL_RADIUS 2.0
*
* Beampipe radius (in cm:)
* (Note some beamipipe radii are taken instead from the optics file,
*   only those with aperture "~" in the optics file take the default dimensions)
BEAMPIPE_RADIUS 1.2
*
* Thickness of beampipe material (in mm)
BEAMPIPE_THICKNESS 2.0
* ================================================
*                   >>> Processes<<<
* -----------     Synchrotron Radiation     -----------
* Flag is true to turn ON Synchrotron radiation:
TURN_ON_SYNCHROTRON 1
*
* Rescale strength of elements due to upstream synchrotron radiation?
RESCALE_DUE_TO_SYNCHROTRON 0
*
* Flag is true to also track the Synchrotron photons
TRACK_SYNCHROTRON_PHOTONS 0
*
* X for Synchrotron radiation lowest energy is X*E_critical
SYNCHROTRON_LOWEST_X 0.
*
* Absolute lowest energy (in MeV) of PROPAGATING synchrotron photons:
SYNCHROTRON_LOWEST_GAMMA_ENERGY 10.0
*
* -----------     Thermal Photons Scattering     -----------
* Flag is true to turn ON scattering of Thermal Planck Radiation
TURN_ON_PLANCK 0
*
* EM Hadronic processes (neutron production):
USE_EM_HADRONIC 0
*
* -----------     Laserwire Parameters     -----------
* laser wavelength (in m):
LASERWIRE_WAVELENGTH 532.0e-9
*
* Laser pointing direction
LASERWIRE_DIR_X 1.0
LASERWIRE_DIR_Y 0.0
LASERWIRE_DIR_Z 0.0
*
* Flag is true to track also the scattered photons.
LASERWIRE_TRACK_PHOTONS 0
*
* ================================================
*                   >>> Backgrounds <<<
* Include scaling so that statistics are more reasonable:
* (one bunch contains ~10^10 particles, so 1000 events (or whatever)
*   should represent this number of particles - hence 10^7:
BACKGROUND_SCALE_FACTOR 1.0
* ================================================
* Muon pair production process
USE_MUON_PAIR_PRODUCTION 1
*
* Scale factor to increase muon production rate (1 => no scaling)
MUON_PRODUCTION_SCALE_FACTOR 100.
```

```
* =================================================
* Use a timer to optimise running?
USE_TIMER 1
*
* =================================================
* Include fields within the iron of elements (for muon scattering etc.)
INCLUDE_IRON_MAG_FIELDS 1
* =================================================
*               Accuracy variables:
* Allowed curvature distance in the chord: (in m)
* for accurate synchrotron tracking:
DELTA_CHORD 1.e-3
*
* Minimum step for chord finder (in m)
CHORD_STEP_MINIMUM 5.e-10
*
* Accuracy of volume intersection (m)
* for accurate tracking:
* DELTA_INTERSECTION 1.e-6
DELTA_INTERSECTION 1.e-9
* =================================================
* print out detailed step information
VERBOSE_STEP 0
* Number of event to print extra info - if zero, then all events printed
VERBOSE_EVENT_NUMBER 0
*
* =================================================
* Whether to use Halo radius in terms of collimation depth
USE_HALO_RADIUS 0
HALO_INNER_RADIUS 0.
HALO_OUTER_RADIUS 0.5
```

12   Acknowledgements

References

[1] GEANT4 collaboration, S. Agostinelli et al.. "GEANT4 - A Simulation Toolkit" (to be published in NIM, 2002.)

[2] S. Redaelli et al., "Comparison of Different Tracking Codes for Beam Delivery Systems of Linear Colliders. " Proc. 8th European Particle Accelerator Conference (EPAC02), CERN-SL-2002-041-AP.

[3] H. Burkhardt, S. Kelner, and R. Kokoulin, "Monte Carlo Generator for Muon Pair Production." CERN-SL-2002-016(AP), CLIC Note 511, May 2002.

[4] P. V. Degtyarenko, M. V. Kossov, H-P. Wellisch Eur. Phys.J. A9 421-424 (2000).

[5] D. Schulte et al. "CLIC Simulations from the Start of the LINAC to the Interaction Point." Proc. 8th European Particle Accelerator Conference (EPAC02), CERN-PS-2002-053-AE, CERN-CLIC-NOTE-531.

[6] G.A.Blair,H. Burkhardt,H-J Schreiber. "Background Simulation for the CLIC Beam Delivery System with Geant." Proc. 8th European Particle Accelerator Conference (EPAC02), CERN-SL-2002-029(AP), CLIC-NOTE-519

[7] "PLACET'' Program, written by D. Schulte, CERN.

[8] P. Tenenbaum, T. Shintake SLAC-PUB-8057 (1999)

[9] G .A Blair, "Simulation of Laserwires at CLIC using BDSIM", Proc. ICFA Nanobeam Workshop, Lausanne (2002).